Advancing the Use of Methane Emission Quantification using TROPOMI Data

MSc Thesis

Simon van Diepen, BSc 4442229

Supervisors

Dr. I. Aben SRON Netherlands Institute for Space Research

Dr. S. Pandey SRON Netherlands Institute for Space Research

Dr. D. M. Stam Delft University of Technology

Image courtesy of S. van Diepen / SRON: Methane increase from 1970 to 2012 (EDGAR).

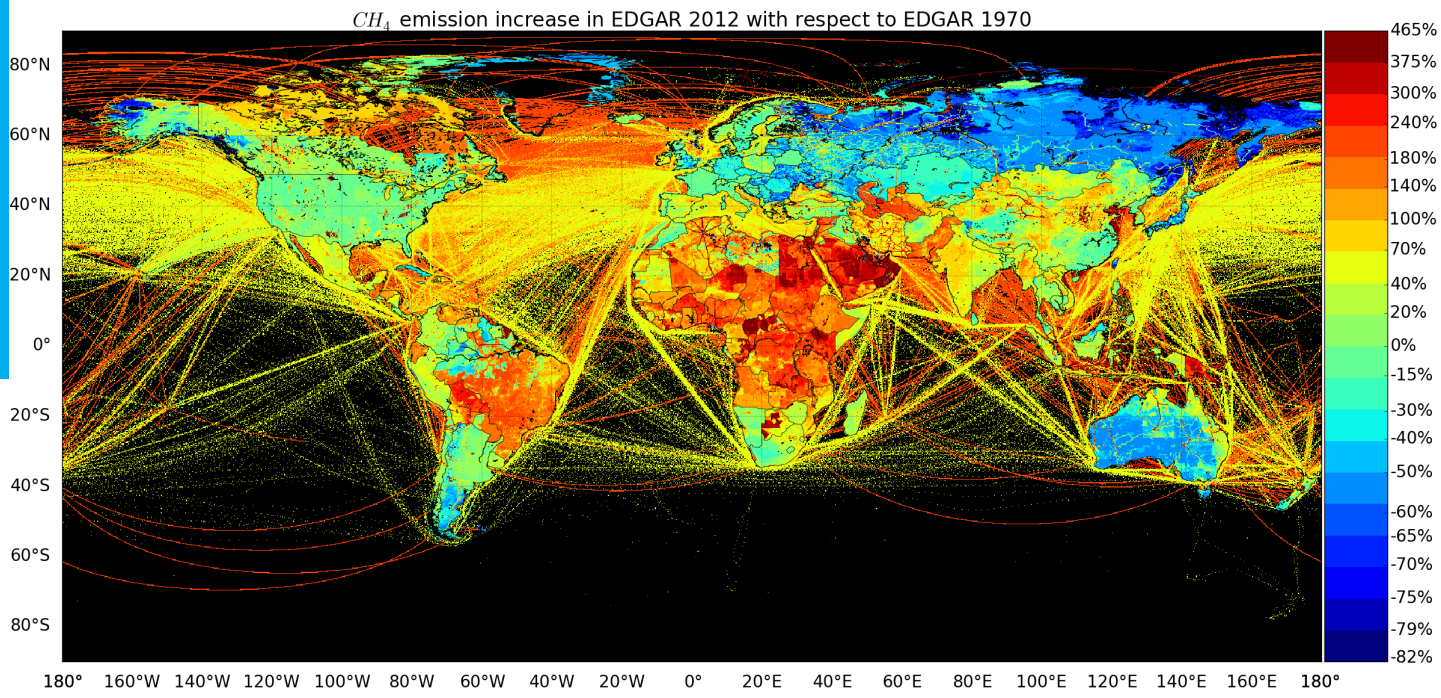

Delft University of Technology

TU Delft Delft University of Technology

SRON Netherlands Institute for Space Research

Challenge the future

CONTENTS

ABSTRACT

Methane is the second-strongest[1] anthropogenic greenhouse gas, with concentrations that have more than doubled since pre-industrial times. Methane could be used for short-term climate change mitigation due to its atmospheric lifespan of 8 to 11 years, while CO_2 stays in the atmosphere for over 100 years. For emission reduction one needs to know how much methane is emitted, and where emissions take place. Currently, 3 satellites provide global measurements of total columns of methane. TROPOMI currently has the best spatio-temporal coverage, as it has daily, near-global coverage at $5.6\times7\text{km}^2$ resolution. Methane retrievals require cloud-free conditions, thus averaging over time is needed for better coverage. One fast, data-driven method for quantification on these time-averaged concentration maps is a mass-balance method developed by Buchwitz *et al.* (2017), but it has a large error estimate of $0.5E + 0.3\text{MtCH}_4\cdot\text{yr}^{-1}$ for a source with emission E. Most sources[2] are smaller than 0.6 $\text{MtCH}_4\cdot\text{yr}^{-1}$, leading to an error estimate larger than 100%. Furthermore, it systematically underestimates emissions by around 40%. The objective of this thesis is to develop a new emission estimation method with a lower error estimate.

One of the main causes of the high error estimate of the method of Buchwitz *et al.* is expected to be neglecting the plume coming from the source moving into the background region. In this thesis this effect is taken into account, together with the wind direction and wind speed.

A WRF atmospheric transport model was run over the continental United States for 1 year. A selection of 33 methane source regions were quantified. Our method gives between 0.81±0.039 and 0.86±0.033 of the true emission rate, while the results of the method of Buchwitz *et al.* show the 40% underestimation (0.63±0.024 of the true emission rate). The estimates of the proposed method do not vary with the background length to source length ratio L_B/L_S, whereas the error of the estimates of the method of Buchwitz *et al.* does decrease with increasing L_B/L_S due to a decreasing influence of the plume on the background. No dependencies on wind speed, latitude, longitude, or source shape were found. Two remaining error sources were quantified: firstly, on time-averaged measurements, we found the wind direction only has an effect of ±4% on the estimates. Therefore the wind direction was fixed to the mean value of this variance. Secondly, the effect of inhomogeneities in the source region was found to be less than 1%. Thirdly, there is a weak dependency on the total emission rate in the background region (r^2=0.3). More research is needed for a correction. The lowest model error estimate found is $\sigma_E = 0.164 \cdot E + 0.002\text{MtCH}_4\cdot\text{yr}^{-1}$ for $L_B/L_S = 3$. The total error estimate also includes the independent wind speed variance and satellite measurement errors.

Compared to the error estimates of Buchwitz *et al.* (2017), taking into account the plume has removed 60-70% of the linear error and 98% of the constant error[3] with an optimum reached for $L_B/L_S = 3$. We find a systematic underestimation of 14-19% using our method, indicating 53-65% of the systematic underestimation is removed. The proposed method works well on both simulations and satellite measurements, where estimates on the latter are consistent with previous estimates in literature. However, large errors in wind speed can deteriorate the error estimate significantly.

The proposed model was then applied to TROPOMI measurements over the Permian oil and gas basin in western Texas and New Mexico, and the Sudd wetlands in South Sudan for 2018 and 2019. The error estimates are a combination of the model error and the wind speed variance. For the Permian the proposed method estimates $4.0\pm0.8\text{MtCH}_4\cdot\text{yr}^{-1}$ in 2018, and $5.1\pm1.0\text{MtCH}_4\cdot\text{yr}^{-1}$ in 2019. Both are consistent with the wind-rotated, cross-sectional flux method employed by Schneising *et al.* (2020) and the atmospheric inverse modelling employed by Zhang *et al.* (2020). For the Sudd wetlands the proposed method estimates $9.0\pm2.4\text{MtCH}_4\cdot\text{yr}^{-1}$ in 2018, and $10.8\pm2.3\text{MtCH}_4\cdot\text{yr}^{-1}$ in 2019, consistent with the variability found by Lunt *et al.* (2019) using a hierarchical Bayesian inversion. In all cases, the variation of the estimated emission when varying L_B/L_S can be attributed to large sources in the background region.

For future work it is recommended to investigate the main error source that has not been quantified yet: sources in the background region. Accounting for this effect will likely improve estimates even more.

[1] The strongest anthropogenic greenhouse gas is carbondioxide (CO_2)

[2] Typical anthropogenic sources include: leakages from oil and gas facilities, coal mines, livestock, and rice cultivation

[3] In our error estimate of $\sigma_E = 0.164 \cdot E + 0.002\text{MtCH}_4\cdot\text{yr}^{-1}$, 0.164 is the linear error and $0.002\text{MtCH}_4\cdot\text{yr}^{-1}$ is the constant error

I

General Introduction

Methane is an important greenhouse gas, responsible for more than half the global warming due to CO_2 with a 200 times lower atmospheric concentration Since pre-industrial times the concentration of methane has more than doubled, leading to methane playing an important role in the enhanced greenhouse effect. Due to its short atmospheric lifetime of 8 to 11 years, methane is very interesting for short-term emission reduction as the resulting effects would be noticeable much sooner than with CO_2, which stays in the atmosphere for over 100 years.

To reduce emissions, however, one first has to know how much emission there is, and where it is located. Since it is infeasible to put groundbased sensors everywhere or measure everywhere using aircraft, satellite sensors are essential. The first satellite sensor measuring methane with sensitivity down to the Earth's surface, SCIAMACHY, became operational in 2003 with a resolution of $30\times60\text{km}^2$. The most recent instrument, TROPOMI, was launched in 2017 with a resolution of $5.6\times7\text{km}^2$ in 2020. TROPOMI also has daily global coverage, giving a wealth of information about methane concentrations worldwide.

Multiple methods exist for methane emission quantification using satellite data. However, all of these have drawbacks, which can mostly be seen in the errors of many methods being very large. Multiple methods are also not applicable for sources without a clear large plume. The mass balance method developed by Buchwitz *et al.* best fits the goal of estimating emissions on time-averages methane total column measurements[1, 2]. The large error estimate of >100% for sources <0.6MtCH_4/yr is the main issue with this method.

The intent of this thesis is to publish the results in a journal. This chapter therefore contains a general introduction for a non-expert audience. Methane itself is explained in more detail in Section I.1. TROPOMI is discussed and compared to other satellites in Section I.2, after which the current methane estimation method is shown in Section I.3. The problem statement is formulated in Section I.4, after which the thesis structure is explained in Section I.5.

I.1. Methane

The CH_4 concentration in the atmosphere is governed by four processes[3, 4]:

- Emissions by sources on the ground. All known sources are listed in Table I.1. The largest sources are wetlands, livestock, and the oil and gas industry.
- Transportation of CH_4 by the wind.
- Chemical reactions in the atmosphere. These are, in the case of CH_4, the sink reactions with hydroxide (OH), and in smaller quantities atomic oxygen (O), atomic chlorine (Cl), and atomic fluorine (F).
- Deposition onto the surface. This happens due to methanotrophic bacteria and in wetlands with variable saturation.

The lifetime of CH_4 in the atmosphere is estimated to be between 8 and 11 years[4]. Due to this relatively long lifetime CH_4 is well-mixed throughout the troposphere, and to a lesser extent, throughout the stratosphere[3]. In the troposphere, variations with latitude in the methane background concentration, X_b, are present. These are mainly caused by transport in the North-South direction taking significantly longer than transport in East-West direction, and that more emission sources are located in the northern hemisphere[3, 5]. Transport around the globe in East-West direction takes up to 2 weeks, whereas transport from 30° latitude to the poles takes around 1 month, from 30° latitude to the equator up to 2 months, and across the equator around 1 year. Vertical mixing into the stratosphere is very slow due to the temperature inversion in the stratosphere: atmospheric layers are stable due the warm air being less dense than the cold air. In the stratosphere, the cold air is already below the warmer air, and therefore buoyancy effects return the air parcels to their original positions. This also means that the troposphere has a higher methane concentration than the stratosphere[5]. Methane sources cause a concentration enhancement relative to this background, which can be measured, as will be discussed in Section I.2[6].

Table I.1: Different Types of Methane Sources[4]

	Thermogenic (organic decomposition under high pressure and heat)	**Biogenic** (anaerobic organic decomposition)	**Pyrogenic** (incomplete combustion)
Anthropogenic	Coal mining Gas and oil industry	Livestock digestion and manure Landfills and waste Rice cultivation	Biomass burning Biofuel burning
Natural	Onshore geological activity Offshore geological activity Oceanic chemical processes	Wetlands Fresh water life forms Wild land animals Termites Permafrost soils Vegetation Oceanic life	Wildfires

The background methane mixing ratio has increased from 700 to 900ppb to about 1800ppb between 1840 (pre-industrial times) and 2000 due to anthropogenic emissions[7, 8]. Global emissions have continued to increase between 2000 and 2014, and currently are at $550 TgCH_4 \cdot yr^{-1}$ (540-568)[4]. To better understand the greenhouse effect of methane, it is useful to compare it to carbondioxide (CO_2). Typical values for the concentration of CO_2 in the atmosphere are around 400ppm, while typical values for the concentration of CH_4 in the atmosphere are around 1.8ppm[9]. This means that the CO_2 mixing ratio is around 200 times higher than the CH_4 mixing ratio. The effect of greenhouse gases on the heating of Earth is measured using radiative forcing, which is defined as the radiative flux change induced by the presence of the gas in the atmosphere[10]. A positive radiative forcing means the troposphere-surface system gains energy and heats, whereas a negative radiative forcing means the system loses energy, and thus cools. The additional radiative forcing of CO_2 is around $1.7 W/m^2$, whereas the additional radiative forcing of CH_4 is $0.97 W/m^2$ relative to pre-industrial times[9]. This means that even though the concentration of CO_2 is 200 times the concentration of CH_4, the radiative forcing is only 1.76 times larger, as methane is a much stronger greenhouse gas on a per molecule basis. With this radiative forcing, CH_4 is the second strongest anthropogenic greenhouse gas. Current emission rate trends are consistent with a radiative forcing of $8.5 W/m^2$ in 2100[4, 8].

The greenhouse effect of CH_4 also causes three positive feedback loops[11]. First, permafrost soils are a source of CH_4[4, 12]. In permafrost soils, around 95% of the emissions originate from thaw lakes, which can increase in frequency, size, and lifetime when temperatures increase due to increasing radiative forcing. Increased CH_4 emissions would cause an even larger increase in radiative forcing, causing more temperature rise, and so on.

Secondly, wetlands will also heat up. Wetland ground layers with a temperature below 0°C cannot emit CH_4[11]. However, when the temperature rises, such ground layers may heat to temperatures above 0°C, causing an increase in CH_4 emissions.

Thirdly, heating of the atmosphere increases the evaporation rate of water in moist soils[13]. The efficiency of CH_4 absorption by methanotrophic bacteria worsens when the soil moisture saturation level drops below around 40%. This sink will therefore decrease in magnitude, causing an increase in CH_4 concentrations in the atmosphere.

I.2. TROPOMI

TROPOMI was launched on 13 October 2017 on board of Sentinel 5-Precursor[6]. The satellite was launched into a polar sun-synchronous orbit with a local overpass time of 13:30. This orbit allows for collaboration with Suomi National Polar-orbiting Partnership (Suomi-NPP), a satellite observing cloud cover in the same orbit with a local overpass time of 13:35. TROPOMI had a resolution at beginning of life of $7x7 km^2$ at nadir, but this has been changed to $5.6x7 km^2$ from 6 August 2019 onwards[14, 15]. This combination of resolution, orbit, and a swath width of around 2600km results in TROPOMI being able to scan the entire globe every day. TROPOMI has an expected lifetime of 7 years.

TROPOMI measures in three spectral ranges: between 270 and 500nm in the UV and visible light, 675 to 775nm in the near infrared, and around 2305 to 2385nm in the SWIR[6]. The latter of these ranges is used for CH_4 measurements. The resolution around 2350nm is 0.25nm. Similar to SCIAMACHY, TROPOMI is a passive imager as it is using sunlight backscattered and reflected by the surface and atmosphere. TROPOMI measurements are found to be in excellent agreement with Greenhouse gases Observing SATellite (GOSAT) measurements, having a mean difference of 13.6ppb with a standard deviation of 19.6ppb[16].

GOSAT is one of the other 3 satellites measuring CH_4, together with GreenHouse Gas SATellite (GHGSAT). GOSAT has very sparse pixels, resulting in multi-year averages being needed for the same results TROPOMI can show in a single overpass[16]. GHGSAT measures at a much higher resolution than TROPOMI (less than $50x50m^2$), but can only measure $12x12km^2$ per orbit (about 100 minutes)[17]. A fourth instrument, SCanning Imaging Absorption SpectroMeter for Atmospheric CHartographY (SCIAMACHY), was aboard ENVIronmental SATellite (ENVISAT), with which contact was lost in 2012[18]. TROPOMI therefore is best suited for investigating current localised methane emissions on a global scale. It is noted that for most applications, time-averages are still required, as measurements need cloudless conditions to be reliable[19].

I.3. Current Methane Quantification Approach

Buchwitz *et al.* developed a method, hereafter the Buchwitz method, with as primary goal to create a simple and fast method for methane emission quantification using satellite observations of total methane columns[1] [2]. Their method is used for quantification on average concentration maps of at least multiple months. This assumption has the intended effect that sufficient coverage is obtained. Due to the long time scales used, one can assume the wind comes equally from all directions, and thus that one can ignore the wind direction.

The Buchwitz method defines a rectangular source region, in which a homogeneous emission E is assumed, as can be seen in Figure I.1. This source region has length L_S in the X-direction and W_S in the Y-direction. Around the source region a background region is drawn with length L_B along X and length W_B along Y. This background region does not need to have the same aspect ratio[2] as the source region. The goal of the method is to find an approximation for the emission E.

Under the assumption that the wind is distributed homogeneously in all directions, the emission enhancement pattern in the background region will be gradually decreasing in every direction the further away from the source, as visualised in Figure I.1. The emission enhancements in the source region on the other hand are constant. These enhancements are added to a background methane concentration, X_b, which is the total concentration CH_4 that would be there without any emissions from the source region. With emissions taken into account, the average concentration CH_4 in the background will be enhanced to $\overline{X}_B$, and the average concentration in the source region to $\overline{X}_S$. Note that the bars above the variables indicate the average of all measurements within the respective region. The most important assumption made by Buchwitz *et al.* is that the enhancement in the background region due to CH_4 emissions in the source region is negligible compared to the normal background concentration, meaning that Equation I.1 holds.

$$\overline{X}_B \approx X_b \tag{I.1}$$

To approximate the average measured concentration in the source region the average wind speed has to be considered. Due to the long time average, the wind angle α is ignored. The average concentration within the source region can then be calculated as per Equation I.2, where τ is the residence time in the source region, or in other words the time it takes for an air parcel to cross the entire source region.

$$\overline{X}_S = X_b + \frac{EF_{CF}}{L_S W_S}\frac{\tau}{2} = X_b + \frac{EF_{CF}}{L_S W_S}\frac{L}{2U} \tag{I.2}$$

where L is the path length through the source region when approached from any direction in m, U the wind speed in $m{\cdot}s^{-1}$, and F_{CF} is a constant conversion factor equal to $1.871{\cdot}10^8 ppb{\cdot}km^2{\cdot}MtCH_4^{-1}$.[2] τ is divided by 2 since the enhancement builds up gradually during the time within the source region: when entering, the enhancement in the air parcel is 0 ppb, whereas it is only at its full strength when leaving the source region. This means the average concentration within the source region is only half of the value of the enhancement when leaving the source region. Combining Equations I.1 and I.2 leads to Equation I.3.

[1] All information in this section is taken from Buchwitz *et al.*[2], unless otherwise noted.

[2] $AR_B = \frac{L_B}{W_B}$, and $AR_S = \frac{L_S}{W_S}$, where A is the aspect ratio.

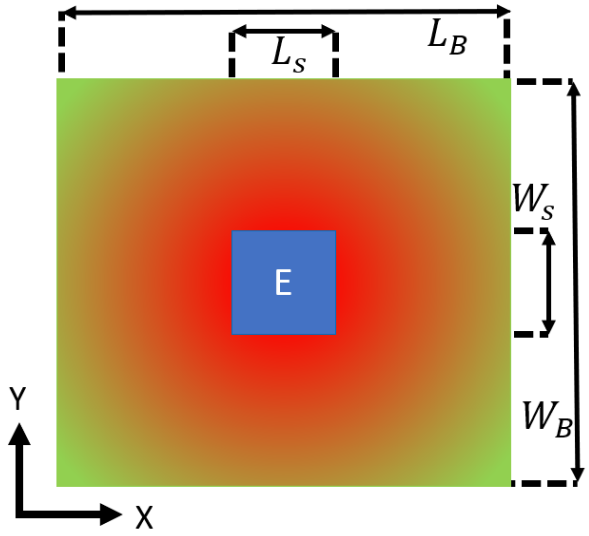

Figure I.1: Geometry for the Buchwitz Method. Red indicates higher XCH_4, while green indicates lower XCH_4.

$$\begin{aligned} \overline{X}_S &= \overline{X}_B + \frac{EC}{L_S W_S}\frac{L}{2U} \\ E &= \frac{L_S W_S}{F_{CF}}\left(\overline{X}_S - \overline{X}_B\right)\frac{2U}{L} \end{aligned} \tag{I.3}$$

The reference length L is defined by Buchwitz *et al.* to be $\sqrt{L_S W_S}$, meaning their final emission quantification equation is Equation I.4.

$$E = \frac{L_S W_S}{F_{CF}}\left(\overline{X}_S - \overline{X}_B\right)\frac{2U}{\sqrt{L_S W_S}} \tag{I.4}$$

I.3.1. Error Estimation

An empirical error estimation was also performed by Buchwitz *et al.* Their 1σ empirical error estimate based on 230 source regions is given as per Equation I.5.

$$\sigma_E = 0.3\frac{MtCH_4}{yr} + 0.5E \tag{I.5}$$

where E is the estimated emission in $MtCH_4 \cdot yr^{-1}$ (Equation I.4). They also report a systematic underestimation of 40% of the source strength. The most important observation from this error estimate is that for sources smaller than $0.6 MtCH_4 \cdot yr^{-1}$ the 1σ error estimate is more than 100%. Since more than 15000 methane emission measurements from 20 studies between 2006 and 2019 in the natural gas industry find leaks of at most $0.1 MtCH_4/yr$, this uncertainty is very significant[20, 21]. It is however to be noted that many of these sources include small leaks which might merge in satellite observations due to resolution constraints, meaning the measured enhancement might be a summation of multiple emissions.

I.3.2. Overview of Assumptions

The assumptions listed below were made by Buchwitz *et al.* during the derivation of Equations I.4 and I.5. Note that not all assumptions have been mentioned earlier.

- Cross-wind dissipation of methane from the source region into the background region is negligible.
- The enhancement plume due to CH_4 emitted in the source region moving in the direction of the wind vector into the background region, is negligible with respect to the background concentration.
- The background concentration is constant over the entire source and background region.

- The wind speed is constant over the entire source region. For this wind speed global statistical averages are assumed to be representative, which is equal to $1.1 \mathrm{m \cdot s^{-1}}$. They arrive at this wind speed by minimising the total sum of quantification errors made over the test cases in their simulation.
- The source region is rectangular.
- The emissions within the source region are homogeneously distributed.
- No other sources and plumes are present in the background region.

I.4. Problem Statement

This thesis will focus on improving the Buchwitz method error estimate. There are a number of important assumptions that can be avoided. The emission estimation problem can also be solved without them in a closed-form equation. Most importantly, I expect the enhancement in the background region due to emissions in the source region to have a large influence on the error estimates. This leads to the research question:

How can the uncertainty of methane emission rate estimates from TROPOMI observations be reduced?

There are two parts to this research question: how can the current methods be improved, and how much improvement can be achieved by doing so. The research question will be solved by starting from the problem formulated by Buchwitz *et al.*[2], and removing the assumptions with a large impact. After this, an atmospheric transport model with known emissions is run to generate artificial data, on which both the Buchwitz method and the newly developed method is applied and compared.

I.5. Thesis Structure

This thesis is directed towards two audiences. Chapter II contains the paper, which is directed towards an expert audience. Within this chapter there is a specialised introduction in **??**, and the description of data and methods in **??**. The results are shown and discussed in **??**[3], after which the conclusion is drawn in **??**. This conclusion is repeated for the non-expert audience in Chapter II, after which recommendations are given in **??**. The derivations of the methods shown in **??** can be found in **??**.

It is intended to publish the results of this thesis in a journal.
The full thesis will therefore become available in the repository after the publication of this paper.

[3] Due to time constraints, the application of the derived equations to TROPOMI data was performed by Sudhanshu Pandey of SRON Netherlands Space Research Organisation. The results obtained by his analysis are shown in **??**.

II

General Conclusion

Methane is the second-strongest anthropogenic greenhouse gas after CO_2, whose atmospheric dry air mole ratios have more than doubled since pre-industrial times. Its emission quantification using satellite-measured concentrations for most applications requires averaging measurements over time due to the need for cloud-free conditions. The current best method for time-averaged concentration measurement maps, proposed by Buchwitz *et al.* (2017), suffers from large errors, especially for small sources: $\sigma_E = 0.5E + 0.3\text{MTCH}_4\cdot\text{yr}^{-1}$. It gives an underestimation of 40% of the true source emission rate. For sources are smaller than $0.6\text{MTCH}_4\cdot\text{yr}^{-1}$, it gives errors larger than 100%. This leads to the problem statement of this thesis:

How can the uncertainty of methane emission rate estimates from TROPOMI observations be reduced?

A new method was designed based on the mass-balance method of Buchwitz *et al.* (2017). This research took the plume coming from the source region moving into the surrounding background region into account, as well as the wind direction. One additional assumption was made to simplify the model: the source region and the background region have the same shape. For time-averaged measurements the wind direction only contributed ±4% to the full estimate, thus its dependency was removed by fixing the wind direction to the angle for which the mean emission rate was estimated. Local wind speeds were used, and an altitude and pressure correction were applied.

To verify our method, a WRF atmospheric transport model was run over the continental United States for 1 year. 33 source regions were selected and their emissions quantified. Our method gives between 0.81±0.039 and 0.86±0.033 of the true emission rate, while the application of the Buchwitz method is consistent with their findings (0.63±0.024 of the true emission rate). The estimates of the proposed method do not vary with L_B/L_S, whereas the estimates of the method of Buchwitz *et al.* do increase with increasing L_B/L_S due to a decreasing influence of the plume on the background. No dependencies on wind speed, latitude, longitude, or source shape were found. There is a weak dependency on the total emission rate in the background region (r^2=0.3), but more research is needed for a correction. The lowest model error estimate found is $\sigma_E = 0.164 \cdot E + 0.002\text{MtCH}_4\cdot\text{yr}^{-1}$ for $L_B/L_S = 3$. The total error estimate also includes the independent wind speed variance and satellite measurement errors, which can be combined using the root-mean-square method.

The proposed model was then applied to TROPOMI measurements over the Permian oil and gas basin in western Texas and New Mexico, and the Sudd wetlands in South Sudan. This was done separately for 2018 and 2019. The error estimates are a combination of the model error and the wind speed variance. For the Permian the proposed method estimates $4.0\pm0.8\text{MtCH}_4\cdot\text{yr}^{-1}$ in 2018, and $5.1\pm1.0\text{MtCH}_4\cdot\text{yr}^{-1}$ in 2019. Both are consistent with Schneising *et al.* (2020) and Zhang *et al.* (2020). The estimates are constant for $L_B/L_S \leq 3$, beyond which large enhancements from the wetlands surrouding the Mississippi river and the urban regions around Mexico City combined with large areas of few measurements over the Gulf of Mexico and the Pacific Ocean decrease the estimates by increasing the average concentration in the background region.

For the Sudd wetlands the proposed method estimates $9.0\pm2.4\text{MtCH}_4\cdot\text{yr}^{-1}$ in 2018, and $10.8\pm2.3\text{MtCH}_4\cdot\text{yr}^{-1}$ in 2019. These estimates are within the uncertainty ranges found by Lunt *et al.* (2019). The estimates in 2019 are constant over L_B/L_S, whereas 2018 shows an increasing linear trend for $L_B/L_S \leq 3.5$, attributed to high enhancements present in southern South Sudan and Uganda. The wind speed variability causes the 2018 error estimate to be higher than that of 2019.

The remaining model errors are caused mostly by four error sources: firstly, there are sources in the background region adding additional enhancements to both regions. Next, the source region was assumed to be homogeneously emitting, which is usually not true. This error was quantified to be less than 1% using the WRF run over the continental United States. Thirdly, the wind direction α was neglected, leading to an error of around 4%. Finally, diffusion was neglected, of which the impact is outside of the scope of this thesis.

To conclude, relative to the error estimates of Buchwitz *et al.* (2017), taking into account the plume has removed 60-70% of the linear error and 98% of the constant error, with an optimum reached for $L_B/L_S = 3$. We find a systematic underestimation of 14-19% using our method, indicating 53-65% of the systematic underestimation is removed. Our proposed method works well on both simulations and satellite measurements, where estimates on the latter are consistent with previous estimates in literature. However, strong variances in wind

speed can deteriorate the error estimate significantly.

For future work a few recommendations are made. There are currently two error sources not accounted for in the model: the emissions in the background region, and diffusion. These error sources are to be quantified for improved estimates. To increase confidence in the method more test cases on TROPOMI data should be run and compared with literature over other areas. This also includes comparison with other emission estimation techniques. While all derivations were done on single measurements, the applications were all time-averages. The performance of both the rectangular and circular equations should be evaluated on single measurements, to see whether their behaviour is still similar. Finally, all regions in this thesis were hand-selected. With TROPOMI measuring the full Earth daily it is impossible to go through all data by hand looking for sources. An automated detection algorithm should be developed for this purpose. These recommendations are listed in **??**.

BIBLIOGRAPHY

[1] S. A. N. van Diepen, *Advancing the Use of Methane Emission Quantification Using TROPOMI Data: MSc Thesis Literature Study,* Delft University of Technology & SRON (2020).

[2] M. Buchwitz, O. Schneising, M. Reuter, J. Heymann, S. Krautwurst, H. Bovensmann, J. P. Burrows, H. Boesch, R. J. Parker, P. Somkuti, R. G. Detmers, O. P. Hasekamp, I. Aben, A. Butz, C. Frankenberg, and A. J. Turner, *Satellite-derived methane hotspot emission estimates using a fast data-driven method,* Atmospheric Chemistry and Physics **17**, 5751 (2017).

[3] D. J. Jacob, *Introduction to Atmospheric Chemistry* (Princeton University Press, 1999).

[4] M. Saunois, P. Bousquet, B. Poulter, A. Peregon, P. Ciais, J. G. Canadell, E. J. Dlugokencky, G. Etiope, D. Bastviken, S. Houweling, G. Janssens-Maenhout, F. N. Tubiello, S. Castaldi, R. B. Jackson, M. Alexe, V. K. Arora, D. J. Beerling, P. Bergamaschi, D. R. Blake, G. Brailsford, V. Brovkin, L. Bruhwiler, C. Crevoisier, P. Crill, K. Covey, C. Curry, C. Frankenberg, N. Gedney, L. Höglund-Isaksson, M. Ishizawa, A. Ito, F. Joos, H.-S. Kim, T. Kleinen, P. Krummel, J.-F. Lamarque, R. Langenfelds, L. Locatelli, T. Machida, S. Maksyutov, K. C. McDonald, J. Marshall, J. R. Melton, I. Morino, V. Naik, S. O'Doherty, F.-J. W. Parmentier, P. K. Patra, C. Peng, S. Peng, G. P. Peters, I. Pison, C. Prigent, R. Prinn, M. Ramonet, W. J. Riley, M. Saito, M. Santini, R. Schroeder, I. J. Simpson, R. Spahni, P. Steele, A. Takizawa, B. F. Thornton, H. Tian, Y. Tohjima, N. Viovy, A. Voulgarakis, M. van Weele, G. R. van der Werf, R. Weiss, C. Wiedinmyer, D. J. Wilton, A. Wiltshire, D. Worthy, D. Wunch, X. Xu, Y. Yoshida, B. Zhang, Z. Zhang, and Q. Zhu, *The global methane budget 2000-2012,* Earth System Science Data **8**, 697 (2016).

[5] A. J. Turner, D. J. Jacob, K. J. Wecht, J. D. Maasakkers, E. Lundgren, A. E. Andrews, S. C. Biraud, H. Boesch, K. W. Bowman, N. M. Deutscher, M. K. Dubey, D. W. T. Griffith, F. Hase, A. Kuze, J. Notholt, H. Ohyama, R. Parker, V. H. Payne, R. Sussmann, C. Sweeney, V. A. Velazco, T. Warneke, P. O. Wennberg, and D. Wunch, *Estimating global and North American methane emissions with high spatial resolution using GOSAT satellite data,* Atmospheric Chemistry and Physics **15**, 7049 (2015).

[6] J. P. Veefkind, I. Aben, K. McMullan, H. Förster, J. de Vries, G. Otter, J. Claas, J. J. Eskes, J. F. de Haan, Q. Kleipool, M. van Weele, O. Hasekamp, R. Hoogeveen, J. Landgraf, R. Snel, P. Tol, P. Ingmann, R. Voors, B. Kruizinga, R. Vink, H. Visser, and P. F. Levelt, *TROPOMI on the ESA Sentinel-5 Precursor: A GMES mission for global observations of the atmospheric composition for climate, air quality and ozone layer applications,* Remote Sensing of Environment **120**, 70 (2012).

[7] G. Rehder, R. S. Keir, E. Suess, and M. Rhein, *Methane in the northern Atlantic controlled by microbial oxidation and atmospheric history,* Geophysical Research Letters **26**, 587 (1999).

[8] J.-F. Lamarque, T. C. Bond, V. Eyring, C. Granier, A. Heil, Z. Klimont, D. Lee, C. Liousse, A. Mieville, B. Owen, M. G. Schultz, D. Shindell, S. J. Smith, E. Stehfest, J. van Aardenne, O. R. Cooper, M. Kainuma, N. Mahowald, J. R. McConnell, V. Naik, K. Riahi, and D. P. van Vuuren, *Historical (1850-2000) gridded anthropogenic and biomass burning emissions of reactive gases and aerosols: methodology and application,* Atmospheric Chemistry and Physics **10**, 7017 (2010).

[9] M. Gytarsky, T. Hiraishi, W. Irving, T. Krug, J. Penman, N. Paciornik, K. Rypdal, A. Garg, W. K. A.-B. T. Pulles, J. Harnisch, K. Paustian, N. H. Ravidranath, A. van Amstel, R. Pipatti, S. M. M. Vieira, *et al.*, *2006 IPCC Guidelines for National Greenhouse Gas Inventories,* Intergovernmental Panel on Climate Change (2006).

[10] V. Ramanswamy, C. Leovy, H. Rodhe, K. Shine, W.-C. Wang, D. Wuebbles, M. Ding, J. A. Edmonds, P. Fraser, K. Grant, C. Johnson, D. Lashof, J. Leggett, J. Lelieveld, M. P. McCormick, A. Oort, M. D. Schwarzkopf, A. Sutera, D. A. Warrilow, and T. Wigley, *Radiative Forcing of Climate,* NASA Scientific Assessment of Ozone Depletion (1991).

[11] B. Ringeval, N. de Noblet-Ducoudré, P. Ciais, P. Bousquet, C. Prigent, F. Papa, and W. B. Rossow, *An attempt to quantify the impact of changes in wetland extent on methane emissions on the seasonal and interannual time scales,* Global Biochemical Cycles **24**, GB2003 (2010).

[12] K. M. Walter, S. A. Zimov, J. P. Chanton, D. Verbyla, and F. S. Chapin-III, *Methane bubbling from Siberian thaw lakes as a positive feedback to climate warming,* Nature **443**, 71 (2006).

[13] M. S. Torn and J. Harte, *Methane consumption by montane soils: implications for positive and negative feedback with climatic change,* Biogeochemistry **32**, 53 (1996).

[14] Koninklijk Nederlands Meteorologisch Instituut Research & Development Satellite Observations, *Mision Status,* `http://www.tropomi.eu/mission-status` (2019), accessed 16 Dec. 2019.

[15] I. Aben and A. Lorente, *Earth Science Group Meeting SRON 03/09/2019,* SRON Internal Presentation (2019).

[16] H. Hu, J. Landgraf, R. Detmers, T. Borsdorff, J. aan de Brugh, I. Aben, A. Butz, and O. Hasekamp, *Toward Global Mapping of Methane With TROPOMI: First Results and Intersatellite Comparison to GOSAT,* Geophysical Research Letters **45**, 3682 (2018).

[17] D. J. Varon, D. J. Jacob, J. McKeever, D. Jervis, B. O. A. Durak, Y. Xia, and Y. Huang, *Quantifying methane point sources from fine-scale satellite observations of atmospheric methane plumes,* Atmospheric Measurement Techniques **11**, 5673 (2018).

[18] ESA, *ENVISAT,* http://www.esa.int/Enabling_Support/Operations/Envisat (2019), accessed 16 Dec. 2019.

[19] A. Butz, A. Galli, O. Hasekamp, J. Landgraf, P. Tol, and I. Aben, *TROPOMI aboard Sentinel-5 Precursor: Prospective performance of CH_4 retrievals for aerosol and cirrus loaded atmospheres,* Remote Sensing of Environment **120**, 267 (2012).

[20] A. R. Brandt, G. A. Heath, and D. Cooley, *Methane Leaks from Natural Gas Systems Follow Extreme Distributions,* Environmental Science & Technology **50**, 12512 (2016).

[21] S. Pandey, S. Houweling, M. Krol, I. Aben, and T. Röckmann, *On the use of satellite-derived CH_4 : CO_2 columns in a joint inversion of CH_4 and CO_2 fluxes,* Atmospheric Chemistry and Physics **15**, 8615 (2015).